Reflow soldering method with gradient energy band generated by optical system

Article *in* Optics Express · October 2018

DOI: 10.1364/OE.26.029203

6 authors, including:

Yongqian Chen
Huazhong University of Science and Technology
16 PUBLICATIONS **61** CITATIONS
SEE PROFILE

Zhu Guangzhi
Huazhong University of Science and Technology
65 PUBLICATIONS **197** CITATIONS
SEE PROFILE

Mu Wang
Huazhong University of Science and Technology
14 PUBLICATIONS **52** CITATIONS
SEE PROFILE

Xiao Zhu
Huazhong University of Science and Technology
63 PUBLICATIONS **327** CITATIONS
SEE PROFILE

Research Article | Vol. 26, No. 22 | 29 Oct 2018 | OPTICS EXPRESS 29203
Optics EXPRESS

Reflow soldering method with gradient energy band generated by optical system

YONGQIAN CHEN,[1,2] GUANGZHI ZHU,[1,2,*] YEBO ZHOU,[1,2] MU WANG,[1,2] XIANSHI JIA,[1,2] AND XIAO ZHU[1,2]

[1]*School of Optical and Electronic Information, Huazhong University of Science and Technology, Wuhan, Hubei 430074, China*
[2]*National Engineering Research Center for Laser Processing, Wuhan, Hubei 430074, China*
[*]*zgzlaser@hust.edu.cn*

Abstract: Laser reflow soldering is an important technology in electronic components processing. In this paper, we presented a simple but efficient method to achieve reflow soldering process with gradient energy band created by just two parallel mirrors. The detailed influence of the variety of optical parameters on the soldering process has been analyzed by using the finite element method. And the modulation of the optical parameters on reflow soldering parameters also has been demonstrated. In our experiment, one HR mirror and one-mirror with transmissivity of 10% have been used to create a gradient energy band with an incident laser power of 50W. In summary, both the simulations and the experiments show that the typical reflow soldering profile has been acquired by the optical system. The high quality joints on both the front and rear surface of the capacitor can be acquired by just one surface radiation of the optical system.

1. Introduction

Reflow soldering technology is widely used in soldering electronic components [1]. Up to now, many methods have been used to achieve the reflow soldering process, such as infrared reflow, vapor phase reflow, laser reflow, etc [2–5]. Laser reflow is an ideal process for attaching heat sensitive devices since the heat is applied only to the area of the joint [6]. Therefore, this technology has been studied in many different areas to achieve high quality soldering and micro soldering [7–9]. On the other hand, in order to increase the production efficiency, soldering equipment is usually assembled in an automatic production line. The electronic components, such as capacitors or resistances, pass through the soldering equipment slowly by the conveyer belt during the soldering process. Figure 1(a) shows a classical reflow soldering machine assembled in an automatic production line. The classical size of the machine is about 6m (length)*0.6m (width). One production line will consume over 200 thousand kilowatt hours each year and the utilization ratio of effective heat energy is very low. Therefore, the reflow soldering equipment usually occupies lots of space and consumes large amount of electrical energies to sustain necessary temperatures [6]. How to reduce the energy consumption and the volume of the equipment have become one of the important subjects for the electronic component packaging enterprise.

The typical reflow soldering process is divided into four standard zones: preheat, soak, reflow and cooling, just as Fig. 1(b) [10].

#331949 https://doi.org/10.1364/OE.26.029203
Journal © 2018 Received 18 May 2018; revised 7 Sep 2018; accepted 28 Sep 2018; published 25 Oct 2018

Optics EXPRESS

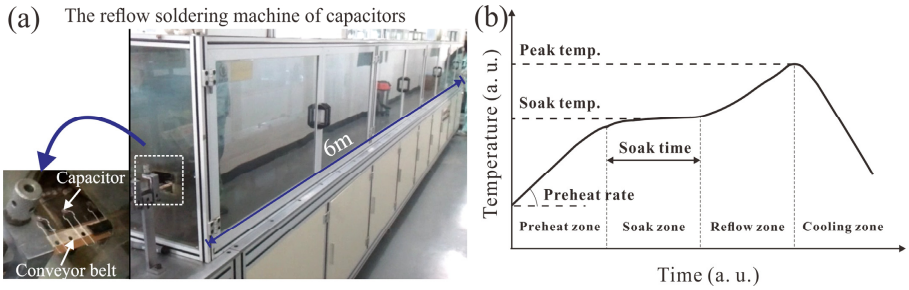

Fig. 1. (a) A classical reflow soldering production line. (b) The temperature profile of a typical reflow soldering process.

In the preheat zone, the temperature of components climbs to the soak temperature linearly in a low preheat rate to release the stress in electronic components. In the soak zone, components are maintained at the soak temperature during the whole zone, and the whole duration is the soak time. During this zone, the oxide layers of both components surfaces and solders are eliminated by the activated flux. In the reflow zone, the temperature rises fast and reaches the peak temperature to melt the solders. Finally, in the cooling zone, the temperature drops to environment temperature and the solders are solidified.

The preheat rate, soak time, soak temperature, and peak temperature are the most important parameters. See Table 1 for implications as below.

Table 1. The description of the parameters in reflow soldering process

Parameter	Definition	Implication
Preheat rate	The average heating rate in the preheat zone	The low preheat rate can ensure the stress in electronic components are released.
Soak time	The duration of the soak zone	The temperature between the components and solders can be converged by choosing the suitable soak time, meanwhile, the oxide can be eliminated in this zone.
Soak temp.	The average temperature of the soak zone	The soak temperature is higher than the flux melting point to evaporate solvents and active the flux.
Peak temp.	The maximum temperature in reflow zone	The peak temperature is higher than the solder melting point to melt solders.

In order to acquire the temperature profile in Fig. 1, traditional laser reflow soldering system has to change the incident laser power with soldering time, during which, electronic components will be fixed on the soldering platform. But this method is no longer suitable for the moving electronic components in production line. Now, a new method based on gradient energy band generated by an optical system is designed to realize the spatial variety of laser energy. In our study, a typical reflow soldering temperature profile can be obtained when electronic components passes through the gradient energy band at a constant velocity.

The outline of this paper is organized as follows. In section 2, the method of generating a gradient energy band is demonstrated at first. Then, the process of acquiring the temperature profile of the capacitor with gradient energy band is analyzed by the finite element method, including the relationship between optical parameters and soldering parameters. At last, a suitable energy band combination and moving velocity of capacitor are obtained. In section 3, experimental setups are built up to verify the simulations in section 2 successfully and following by the test and conclusion. The results demonstrate that not only the reflow soldering process can be achieved, but also the high quality joints can be acquired by our system.

2. Theoretical analysis

2.1 The optical system for obtaining gradient energy band

Figure 2 shows the principle of the gradient energy band generated by two parallel rectangular mirrors. M1 is a mirror with high reflectivity of R_1. M2 is a mirror with a transmissivity of T_2. Firstly, a laser source with an output power P_0 is collimated and penetrated into the sur-

Optics EXPRESS

face of M2 with the incident angle θ. At this time, the incident beam is split into one reflected beam and one transmitted beam. The transmitted beam transmits through M2 with power $P_0 \cdot T_2$ and forms a laser beam spot (the 1st spot) on the soldering plane. The reflected beam is reflected by M2 with power $P_0(1\text{-}T_2)$ and go back to M1. Subsequently, the 1st reflected laser beam is reflected by M1 and then incidents to M2 with power $P_0R_1(1\text{-}T_2)$, this beam will be split into two sub-beams again. One of them transmits through M2 with power $P_0R_1T_2(1\text{-}T_2)$ and forms the 2nd laser beam spot on soldering plane. The other is reflected back to M1. The laser beam will be reflected between M1 and M2 repeatedly. Finally, a row of laser beam spots are generated on soldering plane as the gradient energy band just as Fig. 2.

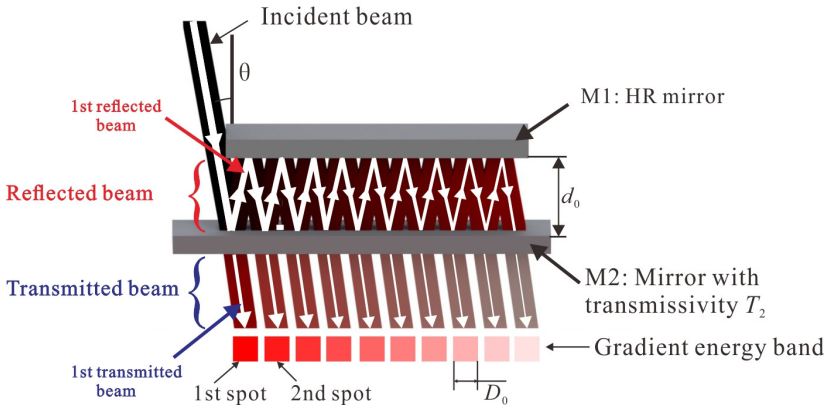

Fig. 2. The schematic picture of the gradient energy band realized by a dual-mirrors optical system.

The power density of the ith laser spot on the soldering plane can be expressed as

$$I_i = \frac{P_0 R_1^{\,i-1} (1-T_2)^{i-1} T_2}{D_0^{\,2}}, \tag{1}$$

where D_0 is the diameter of each laser spot. In order to eliminate the gaps between the spots, the incident angle must be set as

$$\theta = \tan^{-1}(2d_0 / D_0), \tag{2}$$

where d_0 is the distance between M1 and M2.

Figure 3 shows the normalized power density distribution of the gradient energy band changes with different transmissivity of M2. With the decreasing of the transmissivity of M2, the normalized power density of the gradient energy band decreases, and the gradient of the power density difference between each spot decreases gradually. Therefore, the heating rate of electronic components can be modulated by changing the transmissivity of M2.

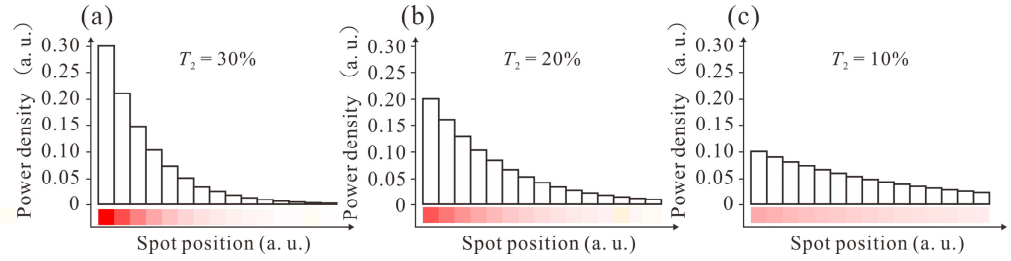

Fig. 3. The relationship between the power density distribution of the gradient energy band and the transmissivity of M2.

Optics EXPRESS

2.2 Thermodynamic model

In our model, the capacitor is used as the soldered component. The capacitor is consist of two pins and one barium oxide ceramic which is shown in Fig. 4. The diameter of the ceramic is 6mm, and the thickness is 3mm. The thin copper films are coated on the front and rear surfaces of the capacitor, the end of pins are coated by Sn-Pb solder and rosin flux. As Fig. 4, the capacitors are located on the soldering plane (XY plane) and moving along the X axis. The gradient energy band is parallel to the x axis. If the capacitor enters gradient energy band from the 1st beam spot, the moving direction is positive direction, otherwise, negative direction.

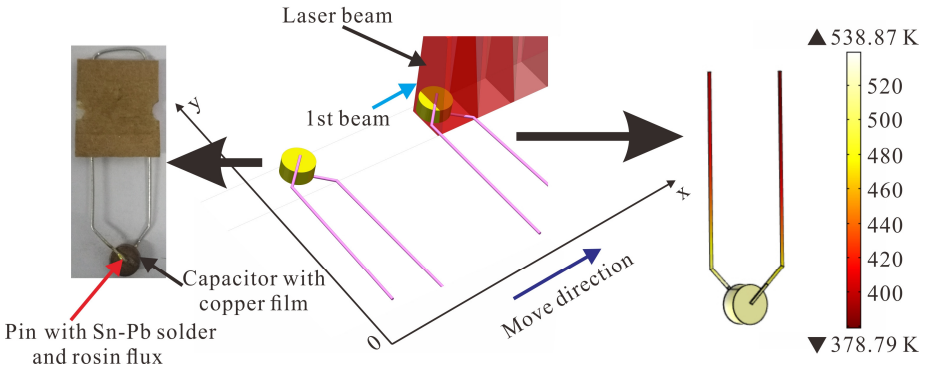

Fig. 4. The model structure of ceramic capacitors soldering with gradient energy band.

In order to describe the soldering process of the moving capacitor, the position of the capacitor passing through the gradient energy band is calibrated by time. The heat transfer equations of the moving capacitor at the solder joint can be described as

$$\begin{cases} \rho_c C_{p-c} \dfrac{\partial T_c(t)}{\partial t} = \nabla\cdot\left(k_c \nabla T_c(t)\right) + Q_c \\ \rho_s C_{p-s} \dfrac{\partial T_s(t)}{\partial t} = \nabla\cdot\left(k_s \nabla T_s(t)\right) + Q_s \\ T_c(0) = T_s(0) = T_{ext} \end{cases}, \tag{3}$$

where ρ is the density, C_p is the specific heat at constant pressure, T is the temperature, k is the thermal conductivity, Q is the absorbed heat power density. T_{ext} is the environment temperature. The subscript "c" and "s" means the parameters of capacitors and Sn-Pb solders, respectively. When the ceramic capacitor passes through the energy band, the boundary conditions of Eqs. (3) can be presented

$$\begin{cases} -\vec{n}_c \cdot\left[-k_c \nabla T_c(t)\right] = h\left[T_{ext} - T_c(t)\right] + \alpha_c I_{las}(t) \\ -\vec{n}_s \cdot\left[-k_s \nabla T_s(t)\right] = h\left[T_{ext} - T_s(t)\right] + \alpha_s I_{las}(t) \end{cases}, \tag{4}$$

where $\vec{n}$ is the normal vector of the boundary, h is the heat transfer coefficient of the air. α is the laser absorption coefficient, I_{las} is the power density incident on the capacitor.

After moving away from the gradient energy band, the temperature of the capacitor will decrease in air convection. The boundary conditions now can be shown as

$$\begin{cases} -\vec{n}_c \cdot\left[k_c \nabla T_c(t)\right] = h\left[T_{ext} - T_c(t)\right] \\ -\vec{n}_s \cdot\left[k_s \nabla T_s(t)\right] = h\left[T_{ext} - T_s(t)\right] \end{cases}. \tag{5}$$

Optics EXPRESS

According to Eqs. (3)-(5), the temperature profile of the capacitor has been calculated by the finite element analysis method with the COMSOL Multiphysics software. The parameters used in the simulation are shown in Table 2.

Table 2. Parameters used in simulation

Parameter	Solder	Copper(with rosin)	Capacitor	Air
thermal conductivity k (W/(m·K))	50	400	6.2	
heat transfer coefficient h (W/m^2·K)				35
Density ρ (g/cm^3)	9	8.7	6.02	–
Specific heat at constant pressure C_p (J/(kg·K))	150	385	430	
Environment temperature T_{ext} (°C)				30
Absorption coefficient α (1/cm)	0.7	0.7		

Figure 5 shows the temperature profile of the capacitor passing through the gradient energy band along positive and negative directions, respectively. When the capacitor moves along the positive direction, the heating rate decreases with soldering time due to the decreasing of energy band gradient. The capacitor temperature increases very fast at first, but the rising rate is getting slower until the heating effect cannot force the convection effect of air. At this time, the temperature reaches the peak, then falls even it is still in the energy band [Fig. 5(a)]. Meanwhile, the heating rate increases with the transmissivity of M2 in the same moving velocity. On the other hand, when the capacitor moves through the energy band along the negative direction, the heating rate of the capacitor increases with soldering time constantly because of the increasing of energy band gradient. The temperature of the capacitor increases faster and faster in the whole process. Moreover, the heating rate increases with the transmissivity of M2, just as Fig. 5(b). Therefore, the heating rate of the electronic component can be modulated by changing transmissivity of M2 to realize highly controllable soldering process.

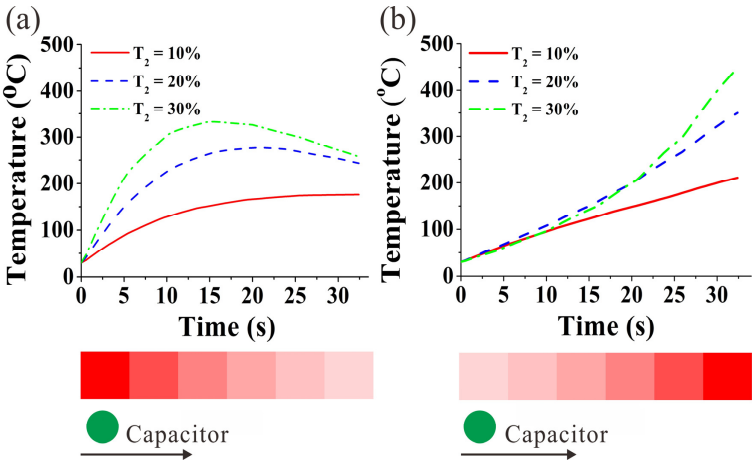

Fig. 5. The temperature profiles in positive (a) and negative (b) direction with different transmissivity of M2 (the incident laser power density is 50W/cm2, the moving velocity is 100mm/min).

In order to realize the typical reflow soldering temperature profile, the suitable combination of different gradient energy bands should be adopted. Figure 6(a)-6(d) show the temperature profile of the capacitor in two gradient energy bands with four different combination methods, respectively. The incident laser power densities are all 50W/cm^2. The moving velocities of capacitors are 100mm/min and the transmissivity of M2 is 20%. Four effective sub-beam spots are used in each energy band.

Optics EXPRESS

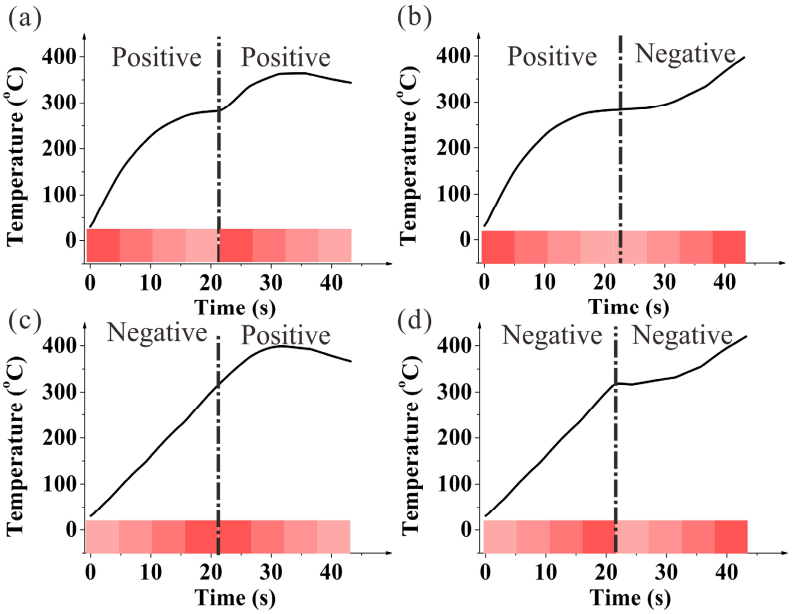

Fig. 6. The temperature profiles of capacitors in different splice sequence model respectively. (a) The positive-positive combination. (b) The positive-negative combination. (c) The negative-positive combination. (d) The negative-negative combination.

Figure 6(a) shows the temperature profile of a capacitor passing through two positive energy bands combination. When the capacitor enters the first positive energy band, the temperature increases quickly at first. Then the heating rate begins to decrease and the temperature keeps stable. This process achieves the preheat zone and the soak zone of the soldering process, respectively. With the capacitor entering the second positive energy band, its temperature increases fast again and reaches the peak to achieve the reflow zone. And then it drops slowly even it still moves in the energy band, just as the last cooling zone in the traditional process, but the cooling rate is lower than that out of the energy band.

Figure. 6(b) shows the temperature profile of the capacitor passing through a positive energy band and a negative band combination. The temperature profile in the first energy band is same to the first zone of Fig. 6(a). When the capacitor enters the negative energy band, the situation is different. The soak stage is longer than that in Fig. 6(a). Enough soak time will help to active the flux. And then the temperature increases to the peak very fast in the reflow zone. Obviously, this temperature profile is similar to the typical reflow soldering such as Fig. 1(b).

Figure 6(c) shows the temperature profile of the capacitor passing through a negative energy band and a positive band combination. When the capacitor enters the negative energy band, its temperature increases quickly constantly and achieves the preheat zone. After it enters the positive energy band, it shows the same path as that in Fig. 6(a). It is obvious that the soak zone in the whole figure disappears. So it is not suitable for reflow soldering.

Figure 6(d) shows the temperature profile of the capacitor passing through two negative bands combination. In the first negative energy band, the temperature profile is the same with Fig. 6(c). And when it enters the second, the profile is the same with Fig. 6(b). In this combination, the four soldering zones can be observed obviously too.

Comparing the four soldering processes, we can find that they can all achieve four soldering zones except Fig. 6(c). Figure 6(b) is close to the typical reflow soldering temperature profile. And Fig. 6(d) fits the “tent style reflow profile” [11]. However, a lower energy utilization appears in the cooling zone in Fig. 6(a). Therefore, both the combination in Fig. 6(b)

Optics EXPRESS

and 6(d) can make good solder joint for electronic components. In this paper, we use the combination as Fig. 6(b) to achieve the reflow soldering process.

In order to analyze the relationship between optical parameters and four soldering zone parameters, some parameters must be redefined based on the temperature profile and shown in the Table 3.

Table 3. Definition of the zones and parameters in gradient energy band reflow soldering process

Soldering zone	Definition	Soldering parameter	Definition
Preheat zone	From beginning to the start of soak zone.	Preheat rate	The average heat rate in preheat zone.
Soak zone	Soak zone is the zone with the temperature T as $\|T-T_{soak}\| \le T_{soak}/9$,	Soak temperature	The temperature for the minimizing heating rate.
Reflow zone	From the end of the soak zone to the peak temperature.	Soak time	The duration of the soak zone is the Soak time.
Cooling zone	From the peak temperature to the end	Peak temperature	The maximum temperature in the whole soldering process.

2.2 Relationship between optical parameters and reflow soldering parameters

Figure 7 shows the relationship between different reflow soldering parameters (preheat rate, soak temperature, peak temperature and soak time) and laser power density in the same moving velocity of 100mm/min with different transmissivity of M2.

Figure 7(a)-7(c) indicate that the preheat rate, soak temperature and peak temperature increase with the incident power density. Based on the same incident power density, the preheat rate, soak temperature and peak temperature increase with the transmissivity of M2. While, the soak time isn't sensitive to power density, just as Fig. 7(d). And the lower the transmissivity of M2, the longer the soak time. But the soak time with the 20% and 30% transmissivity are close to each other.

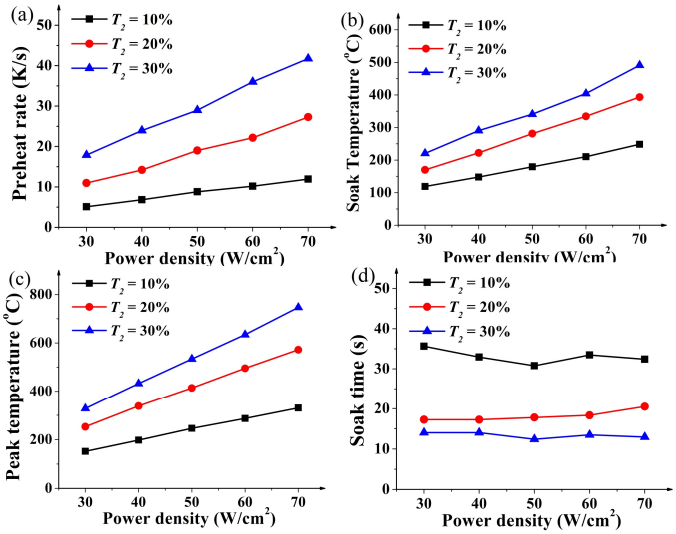

Fig. 7. (a), (b), (c) and (d) describe the relationship between the incident laser power density and preheat rate, soak temperature, peak temperature, soak time with different transmissivity of M2, respectively. In this condition, the velocity of the capacitor keeps at 100mm/min.

Optics EXPRESS

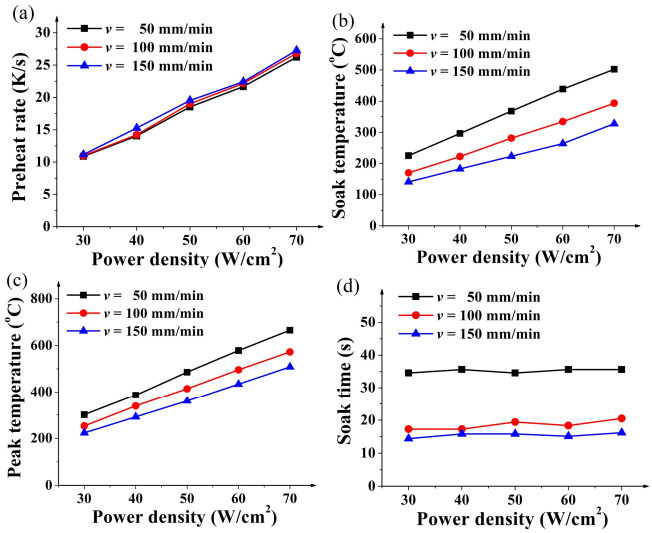

Fig. 8. (a), (b), (c) and (d) describe the relationship between the incident laser power density and preheat rate, soak temperature, peak temperature, soak time with different velocity of the capacitor, respectively. In this condition, the transmissivity of M2 keeps at 20%.

Figure 8 shows the relationship between different soldering parameters and incident power density in different moving velocity. The transmissivity of M2 is 20%. Figure 8(a)-8(c) indicate that the preheat rate, soak temperature and peak temperature increase with the incident power density. While the preheat rate doesn't change much in different moving velocity. And in Fig. 8(d), the soak time keeps stable in different power density. Inversely, the soak temperature, the peak temperature and the soak time decrease with the moving velocity, which is due to the negative correlation between the heating time and the moving velocity.

Figure 9 shows the relationship between different reflow soldering parameters and the moving velocity in the same incident power density of 50W/cm^2 with different transmissivity of M2. In the preheat zone, the preheat rate almost keeps invariant in different velocity. Meanwhile, the preheat rate increases with the transmissivity of M2 for the invariable moving velocity [Fig. 9(a)]. Figure 9(b) and 9(c) are similar to each other, both the soak temperature and the peak temperature decrease with the moving velocity. At the same time, the temperature increases with the transmissivity of M2 for a settled velocity. Figure 9(d) describes that the soak time decreases with the moving velocity, but there are fluctuations due to air conviction.

Optics EXPRESS

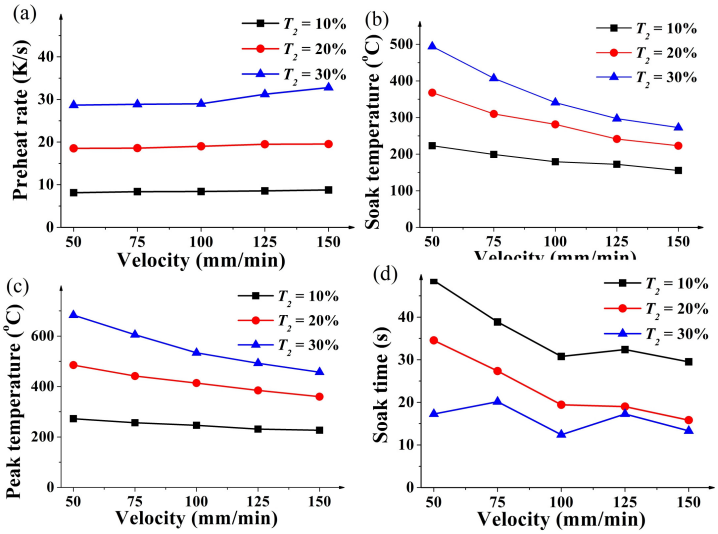

Fig. 9. (a), (b), (c) and (d) describe the relationship between velocity of the capacitor and the preheat rate, the soak temperature, the peak temperature and the soak time with different transmission of M2, respectively. In this condition, the incident laser power density keeps at 50 W/cm^2.

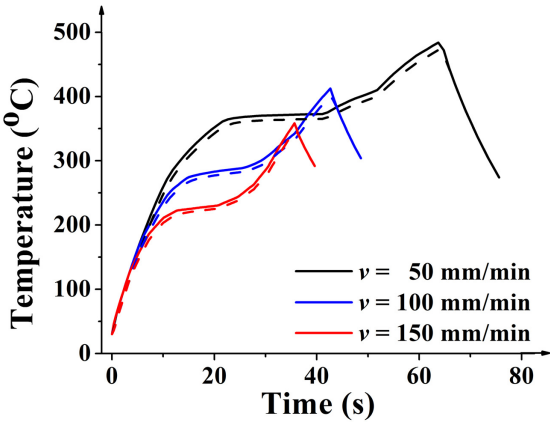

Fig. 10. The temperature profiles of capacitors with the M2 transmissivity of 20%, the incident laser power density of 50W/cm^2. The solid lines represent the front surface, and the dash lines represent the back surface.

Figure 10 shows the temperature profiles of the reflow soldering process for the solder (Sn-Pb) on both front and rear surface of the capacitor in different moving velocity. The solid lines describe the temperature of the solder on the front surface, and dash lines describe that on the rear. The solder temperature on both surfaces are almost the same. Therefore, the two pins can be soldered on both surfaces simultaneously. And the reflow soldering duration reduces with the moving speed obviously implied in Fig. 10.

3. Experimental setup

Figure 11 shows the experimental setup of the gradient energy band reflow soldering system. The gradient energy band was generated by two rectangular mirrors. M1 is a 2 mm thickness mirror with the reflectivity > 99.5% at 940 nm, and the size is 100mm × 40mm. M2 is the output mirror parallel to M1 with the transmission of 10%, 20% and 30%, respectively. The size of M1 and M2 are same. A fiber coupled 940nm diode laser with 50W output power is used as the heating source. In order to increase the uniformity on the soldering plane, the laser

Optics EXPRESS

beam was coupled into a square homogenizing fiber with 0.6mm × 0.6mm cross section at first [12] and then collimated to the size of 9.6mm. The capacitors used in the experiment was the barium oxide ceramic capacitor with two pins, the solder was the Sn63Pb37, and the flux was the rosin. The capacitor was held between the pins, which were fixed on a computerized numerical control (CNC) translation platform during the soldering process, just as the status of the production line. The moving velocity was controlled by the CNC software. An infrared thermal imager (Testo 890-2) was used to record the temperature profile of the moving capacitor during the whole soldering process. The imager has the autofocus function. The distance between the imager and the capacitor was about 60 cm. The horizontal angle was about 45 degree. The time rate of the imager during the recording process is 11 frames per second, and the instantaneous field of view (IFOV) was 1.13 mrad. The emissivity of the imager was 0.7 [13], and the apparent reflected temperature was 20 °C. According to Fig. 6(b), the capacitor entered the energy band from left to right [Fig. 12] at first. In order to simulate the two energy bands splicing situation, the capacitor moved back to the starting point with the same velocity after passing through gradient energy band through the positive one. Figure 12 shows the space distribution of the gradient energy band in different transmissivity of M2, which is similar with the theoretical results in Fig. 2. Therefore, the gradient and distance of the energy band can be modulated by the transmissivity of the output mirror effectively.

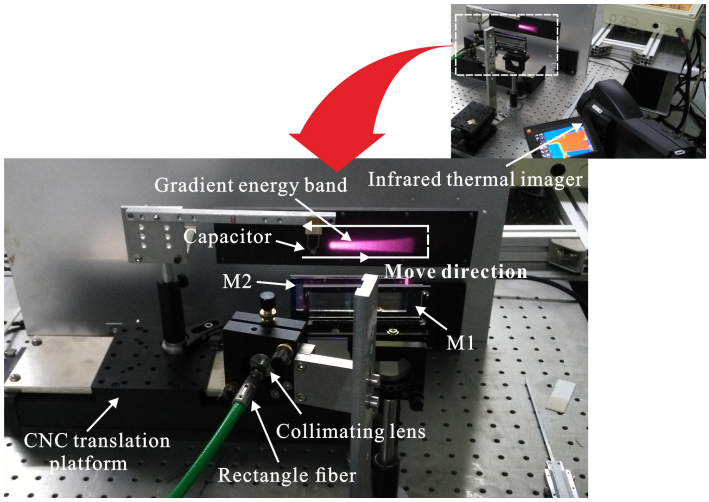

Fig. 11. The experiment scheme photograph.

The returning position is an important parameter in the “backtracking” movement. When the capacitor moves from left to right, we define the returning position as where the temperature begins cooling. Thus, the temperature at the returning position is the soak temperature in the reflow soldering process. Table 4 shows the measured returning position for different transmissivity of output mirrors.

Optics EXPRESS

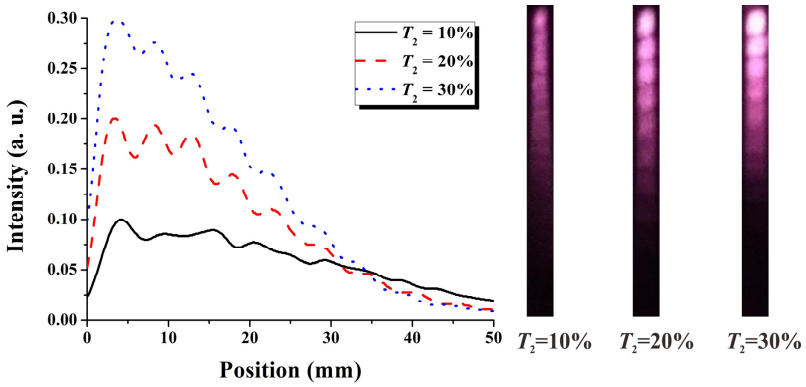

Fig. 12. Energy distribution of energy bands for different transmissivity on the soldering plane.

Table 4. The returning positions for different transmissivity

Transmissivity	Returning position
10%	62 mm
20%	50 mm
30%	34 mm

Secondly, the suitable moving velocity and transmissivity of output mirror will be determined based on the reflow soldering demands of the capacitor, the solders and the flux. Figure 13(a)-13(c) show the relationship between the soak temperature and the moving velocity of the different incident power when the transmissivity is 10%, 20% and 30%, respectively. The error bars are the standard deviation of data. The solid line is the typical soak temperature of rosin flux in 150°C. It shows that several combined parameters can reach typical soak temperature, which has been marked out in Fig. 13(d).

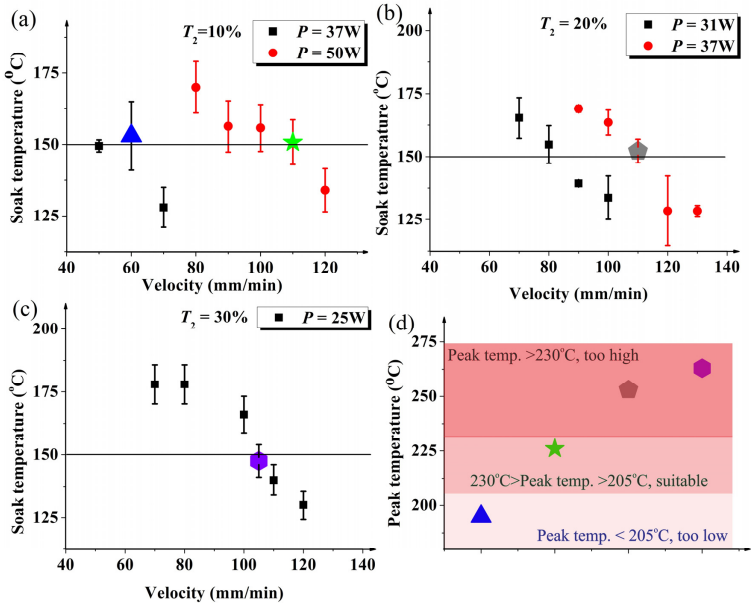

Fig. 13. The relationship between maximum temperatures and capacitor velocity with different laser power during single path movement of capacitor.

On the other hand, in order to simulate the real soldering process in production line, the return velocity of the capacitor must be the same as the positive moving speed. When the capacitor is moving back to the end of the energy band, the temperature of capacitor must reach

Optics EXPRESS

205~230°C, which is the typical temperature of Sn-Pb solder [Fig. 13(d)]. So the optimal combined parameters can be acquired in Table 5.

Table 5. Parameters of the reflow soldering system

Transmission	V_1 (mm/min)	Laser power (W)
10%	110	50

Figure 14 shows the temperature profile of the capacitor moving in the gradient energy band which measured by infrared thermal imager. In this profile, the preheat rate is 6°C/s, the soak time is 17s, the soak temperature is 150°C, and the peak temperature is 225°C. Considering the error by the experimental method, 50 samples are used. The final temperature profile is illustrated in Fig. 14, the square points are the data points, and the solid line is the simulated result, error bars are the standard deviation of data. For the typical Sn-Pb solder, the maximum temperature is 205~230°C. The experimental results indicated that, the typical reflow soldering profile can be acquired accurately by this method.

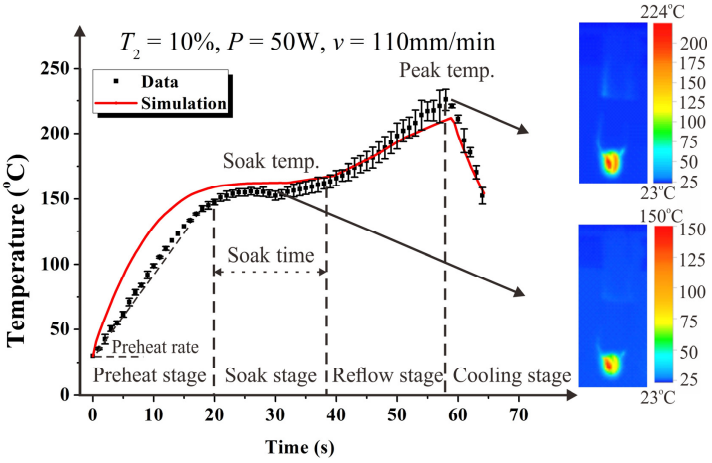

Fig. 14. The temperature profile of the capacitor.

On the other hand, the rear surface of the capacitor can be soldered simultaneously. Figure 15 shows the section metallographic graph of the both surfaces of the capacitor. From the metallograph, the smooth joints have been acquired on both surfaces, and there are no obvious bubbles in the interface between the Barium oxide substrate and the Sn-Pb solder. The results imply that the high quality solder joints have been acquired on both surfaces through one-surface reflow soldering process.

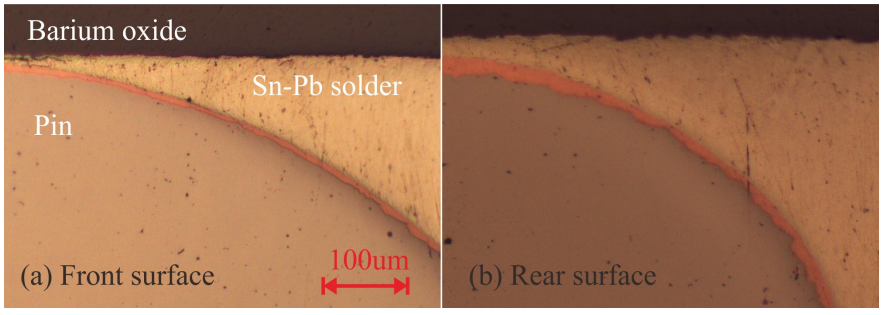

Fig. 15. The metallograph of the joints, the magnification is 200.

Conclusions

To summarize, a new kind of reflow soldering method with a simple structure and compact device is described in the paper. In our paper, we generated different kinds of energy bands

Optics EXPRESS

according to an optical system, and combined them together as a new heating source to acquire the reflow soldering process. Thermodynamic models are built to analyze the relationship between reflow soldering parameters and optical parameters of the gradient energy band. The analytical results show the suitable gradient energy bands combination can make the typical reflow soldering temperature profile for different solders. Based on the optimal design, the experiments are carried out on the ceramic capacitor of barium oxide with a constant moving velocity. Not only the typical reflow soldering temperature profile can be achieved, but also high quality double-surface soldering of the capacitor can be made by using the method. With the same production efficiency, the energy consumption can be saved 50% to 60%, and the volume can be reduced 50% comparing with the existing machine by using the gradient energy band laser soldering technology.

Funding

National Natural Science Foundation of China (NSFC) (61475057); Fundamental Research Funds for the Central Universities (HUST: 2016YXMS213); National Key Research and Development Plan (2016YFE0202500).

References

1. M. R. Harrison, J. H. Vincent, and H. A. H. Steen, "Lead-free reflow soldering for electronics assembly," Solder. Surf. Mt. Technol. **13**(3), 21–38 (2001).
2. C. Anguiano, M. Félix, A. Medel, M. Bravo, D. Salazar, and H. Márquez, "Study of heating capacity of focused IR light soldering systems," Opt. Express **21**(20), 23851–23865 (2013).
3. L. Livovsky, A. Pietrikvoa, and J. Durisin, "Monitoring of the temperature profile of vapour phase reflow soldering," *proceeding of IEEE on International Spring Seminar on Electronics Technology*(IEEE, 2009), pp. 667–669.
4. J. Lee, Y. Lee, and Y. Kim, "Fluxless laser reflow bumping of Sn-Pb eutectic solder," Scr. Mater. **42**(8), 789–793 (2000).
5. B. Illés, "Distribution of the heat transfer coefficient in convection reflow oven," Appl. Therm. Eng. **30**(13), 1523–1530 (2010).
6. N. Lee, *Reflow Soldering Processes and Troubleshooting: SMT, BGA, CSP and Flip Chip Technologies* (Newnes, 2002) Chap. 4.
7. J. Kim, J. Jung, J. Lee, H. Jeong-Suh, and H.-S. Kang, "Effects of Laser Parameters on the Characteristics of a Sn-3.5 wt.%Ag Solder Joint," Met. Mater. Int. **15**(1), 119–123 (2009).
8. W. Liu, Y. Tian, L. Yang, C. Wang, and L. Sun, "Oxidation and Au-Sn reaction of laser reflowed micro-solder joints protected by N_2 or exposed to air atmosphere," Solder. Surf. Mt. Technol. **11**(1), 13–20 (8) (1999).
9. W. Liu, C. Wang, Y. Tian, and L. Kong, "Sagging Phenomenon of Micro-Solder Joints Fabricated by Laser Reflow Process," in *proceeding of IEEE on International Conference on Electronic Packaging Technology* (IEEE, 2007), pp.1–5.
10. J. Gao, Y. Wu, and H. Ding, "Thermal profiling: a reflow process based on the heating factor," Solder. Surf. Mt. Technol. **20**(4), 20–27 (2008).
11. N. Lee, "Optimizing the reflow profile via defect mechanism analysis," Surf. Mt. Tech. **13**(3), 21–38 (2001).
12. G. Zhu, X. Zhu, and C. Zhu, "Analytical approach of laser beam propagation in the hollow polygonal light pipe," Appl. Opt. **52**(23), 5619–5630 (2013).
13. H. Ye, C. Basaran, and D. Hopkins, "Thermomigration in Pb-Sn solder joints under joule heating during electric current stressing," Appl. Phys. Lett. **82**(7), 1045–1047 (2003).